J. DZIK*, A. LISIŃSKA-CZEKAJ*, A. ZARYCKA*, D. CZEKAJ*

STUDY OF PHASE AND CHEMICAL COMPOSITION OF $Bi_{1-x}Nd_xFeO_3$ POWDERS DERIVED BY PRESSURELESS SINTERING

BADANIE SKŁADU FAZOWEGO ORAZ CHEMICZNEGO PROSZKÓW $Bi_{1-x}Nd_xFeO_3$ SPIEKANYCH SWOBODNIE

In the present paper studies on $Bi_{1-x}Nd_xFeO_3$ for x =0.1-0.4 are reported. The mixed oxide method followed with pressureless sintering was employed for ceramics fabrication. Thermal behavior of stoichiometric mixtures of simple oxide powders, viz. Bi_2O_3, Nd_2O_3 and Fe_2O_3 was studied by simultaneous thermal analysis. It was found that with an increase in neodymium content the weight loss increased from 0.75% to 3.16% for x =0.1 and x =0.4, respectively. It was found that weight loss took place mainly within two temperature ranges, namely $\Delta T_1 \approx$ (300-400)^{0}C and $\Delta T_2 \approx$ (600-800)^{0}C. $Bi_{1-x}Nd_xFeO_3$ ceramics was studied in terms of its phase composition (X-ray phase analysis) and chemical composition (EDS method) at room temperature. It was found that $Bi_{1-x}Nd_xFeO_3$ suffered structural phase transition from rhombohedral to orthorhombic symmetry with an increase in neodymium concentration x within the range x =(0.2-0.3).

Keywords: $BiFeO_3$ ceramics, Nd^{3+} doping, X-ray phase and structural analysis

W niniejszej pracy zaprezentowano wyniki badań ceramiki $Bi_{1-x}Nd_xFeO_3$ dla x =0,1-0,4. Do wytworzenia ceramiki zastosowano metodę reakcji w fazie stałej z mieszaniny tlenków wyjściowych Bi_2O_3, Nd_2O_3 i Fe_2O_3 spiekanej swobodnie w atmosferze powietrza. Analiza termiczna stechiometrycznej mieszaniny proszków wykazała wzrost ubytku masy proszku przy wzroście zawartości (x) neodymu w mieszaninie (od 0,75% do 3,16% dla x =0,1 i x =0,4 odpowiednio). Stwierdzono, że ubytek masy zachodzi głównie w dwóch zakresach temperatury, a mianowicie $\Delta T_1 \approx$ (300-400)°C i $\Delta T_2 \approx$ (600-800)°C. Ceramika $Bi_{1-x}Nd_xFeO_3$ została poddana charakterystyce składu fazowego (rentgenowska analiza fazowa) oraz składu chemicznego (metoda EDS) w temperaturze pokojowej. Stwierdzono, że $Bi_{1-x}Nd_xFeO_3$ przejawia strukturalną przemianę fazową z fazy romboedrycznej do rombowej przy wzroście koncentracji neodymu w zakresie x =(0.2-0.3).

1. Introduction

Bismuth ferrite is one of the very few multiferroic materials with a simultaneous existence of ferroelectric (Curie temperature T_C =810-830^{0}C) and antiferromagnetic (Néel temperature T_N = 370^{0}C) order parameters in perovskite structure. $BiFeO_3$ has a rhombohedrally distorted perovskite structure belonging to a space group of *R3c* [1]. The study of these materials is now extremely active and has already given a lot of spectacular results, because of its possible novel applications in the field of radio, television, microwave and satellite communications, audio-video and digital recording and as permanent magnets [2]. So far, bismuth ferrite powders have been prepared by the solid-state methods, such as classic [3, 4] spark plasma sintering [5], mechanochemical methods and solution chemistry methods such as precipitation/co-precipitation [6], sol-gel [7, 8] and hydrothermal [9].

Previous studies have demonstrated that synthesis of pure $BiFeO_3$ bismuth ferrite phase in a form of bulk ceramics is not a trivial task. During its preparation additional (i.e. impurity) phases such as $Bi_2Fe_4O_9$ [3], $Bi_{36}Fe_{24}O_{57}$ [10] or $Bi_{25}FeO_{39}$ [11] appear very often. One of the ways that lead to decreasing formation of impurity bismuth iron oxides and favor formation of single-phase material is to dope bismuth ferrite with neodymium [4, 12]. It is known [13] that by substituting rare-earth cations for A-site Bi^{3+} ion in the nominal $BiFeO_3$ composition, one can effectively modulate the crystal structure parameters of $BiFeO_3$, destroy the space – modulated spin structure, and release the measurement of weak ferromagnetism.

In the present study $Bi_{1-x}Nd_xFeO_3$ for x =0.1-0.4 powders were synthesized using mixed oxide method. The synthesized powders were characterized by scanning electron microscopy and X-ray diffraction method to extract information on their morphology, chemical and phase composition as well as crystal structure.

2. Experimental

The mixed oxide method was employed for the ceramics fabrication. The process of fabrication was described by us elsewhere [4, 12]. Therefore, let us only briefly mention that the stoichiometric mixture of powders was subjected to

* UNIVERSITY OF SILESIA, DEPARTMENT OF MATERIALS SCIENCE, 2 ŚNIEŻNA ST., 41-200 SOSNOWIEC, POLAND

grinding in a planetary ball mill for 24h. The synthesis was carried out at $T = 750°C$ in corundum crucible with air atmosphere for 10h. After synthesis the material was milled in a wet medium. After that it was dried and pressed into pellets under pressure of $p = 60MPa$. The sintering was carried out in ambient air at temperature $T = 1000°C$ for 24h. The flowchart of the complete fabrication process is shown in Fig. 1.

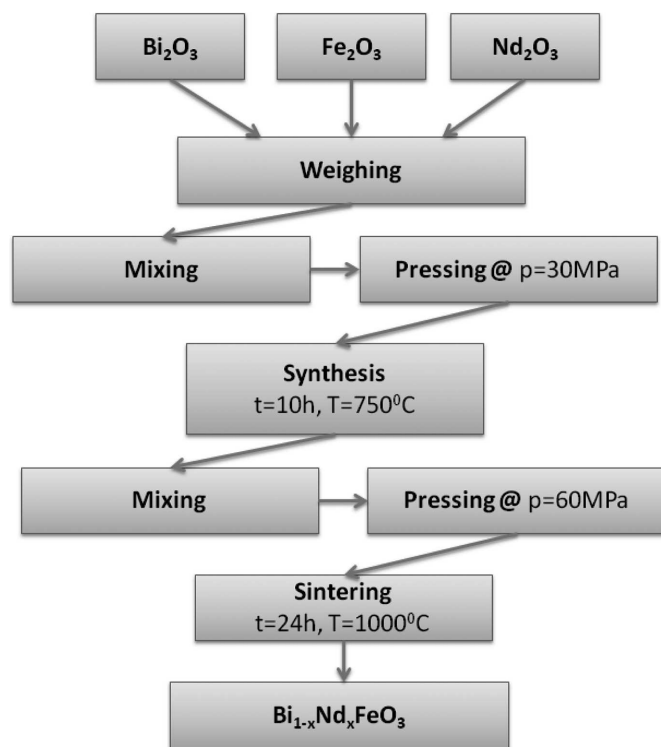Fig. 1. The flowchart of fabrication process of $Bi_{1-x}Nd_xFeO_3$ ceramics

In order to determine the thermochemical properties of $Bi_{1-x}Nd_xFeO_3$ powder differential thermal analysis (DTA) and thermogravimetric analysis (TG/DTG) were used. Simultaneous DTA/TG/DTG measurements were executed by heating the stoichiometric mixture of initial oxide powders in ambient air at the heating rate of $10°C/min$ up to $T = 1000°C$. The morphology of $Bi_{1-x}Nd_xFeO_3$ ceramic samples as well as their chemical composition was studied by scanning electron microscopy, using a scanning microscope HITACHI S-4700 with system of microanalysis EDS-NORAN Vantage.

The powders were subsequently examined by X-ray diffraction method (XRD; Philips PW 3710), using CuKα radiation (detector scan step $\Delta 2\Theta = 0.010$ and a counting time t=7s) at room temperature to identify the phases formed in result of the thermal treatment. Phase analysis of the X-ray diffraction patterns of $Bi_{1-x}Nd_xFeO_3$ powder was carried out using a Match! (Crystal Impact) computer program [14] which now uses facilities of well-known software FullProf [15]. Crystallographic databases ICSD, ICDD and AMCSD/COD were used. PowderCell [16] computer program was utilized for building models of the crystal structure of the new compounds.

3. Results and Discussion

Thermogravimetric (TG) plots (Fig. 2) show that neodymium concentration had an influence on the total weight loss of the reacting powders. With an increase in the content of neodymium dopant the weight loss increases from 0.75wt% up to 3.16wt% for Nd content $x = 0.1$ to $x = 0.4$ respectively. One can see from Fig. 2 and Fig. 3 that there are at least two temperature ranges showing maximal rates of the mass loss, namely $\Delta T_1 \approx (300\text{-}400)°C$ and $\Delta T_2 \approx (600\text{-}800)°C$. At temperature $T > 800°C$ no mass change effects occurred. It is worth noting, that absolute maximal value (i.e. peak value) of DTG minimum (Fig. 3) increases (i.e. from 0.06%/min to 0.20%/min within the range ΔT_1) and shifts toward higher temperature (i.e. from $T = 635°C$ to $T = 681°C$ within the range ΔT_2) with an increase in neodymium content (Fig. 3). From the practical point of view both Fig. 2 and Fig. 3 help to choose the appropriate rate of the thermal treatment of the material under study.
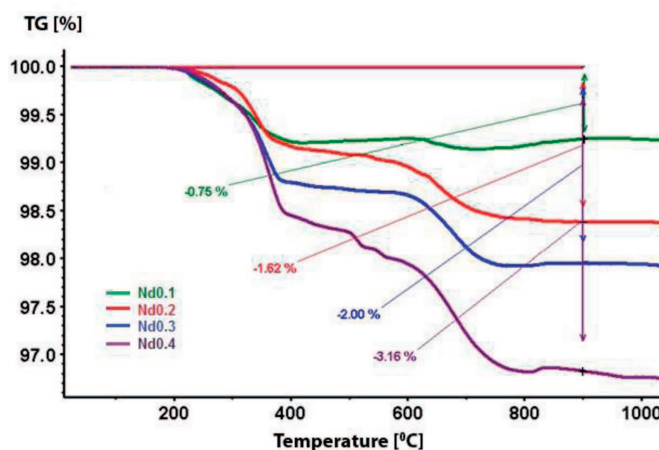

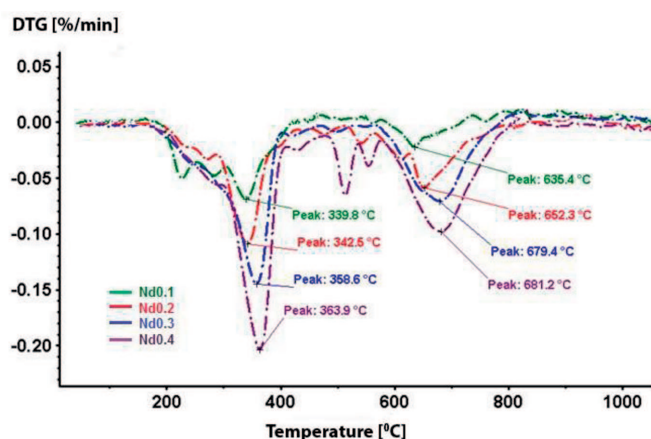Fig. 2. Termogravimetric (TG) curves for stoichiometric mixtures of oxides used for synthesis of $Bi_{1-x}Nd_xFeO_3$ ceramics

Fig. 3. DTG curves for the oxide mixture of $Bi_{1-x}Nd_xFeO_3$

One can ascribe the observed weight loss with evaporation of products and/or by-products of chemical reactions as well as evaporation of Bi_2O_3 oxide. Comparing TG/DTG data (Fig. 3) with DTA behavior (Fig. 4) of the stoichiometric mixture of oxides one can see that at the temperature range ΔT_1 corresponding to the first part of mass loss the exothermic

peaks appeared on DTA curves. It indicates that a chemical reaction took place in the mixture of oxides. On the other hand, taking into account thermal behavior of Bi_2O_3, e.g. reported by us elsewhere [e.g. 17], one can conclude that at the initial stage of heating (i.e. $T < 400°C$) Bi_2O_3 oxide loses about 2wt% of its initial mass. The next temperature range ΔT_2 of the mass loss corresponds to the wide shoulder of possible DTA peak. In this temperature region it is highly possible a phase transition from monoclinic δ-Bi_2O_3 phase to the high temperature cubic phase (at approximately $T = 730°C$) as well as formation of bismuth iron oxide phases.
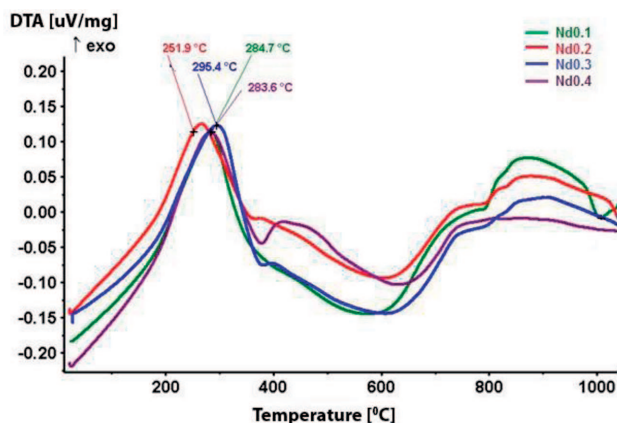

Fig. 4. Differential thermal analysis (DTA) curves for stoichiometric mixtures of oxides used for synthesis of $Bi_{1-x}Nd_xFeO_3$

EDS spectra and SEM photographs (the insets) showing morphology of fracture for $Bi_{1-x}Nd_xFeO_3$ ceramics are presented in Fig. 5. One can see from SEM pictures that concentration of neodymium had an effect on particle size. An increase in neodymium content caused a decrease in the average size of the grains.

Theoretical and experimental content of elements (calculation for simple oxides) for $Bi_{1-x}Nd_xFeO_3$ ceramics is given in Tab. 1. One can see that small deviations from the theoretical composition have occurred but they do not exceed a value of 4.8%. It is consistent with the resolution of the utilized method of investigation.

Phase analysis was performed for X-ray diffraction patterns of $Bi_{1-x}Nd_xFeO_3$ powders fabricated in the present

research. As an example results of qualitative analysis for $Bi_{0.9}Nd_{0.1}FeO_3$ and $Bi_{0.6}Nd_{0.4}FeO_3$ are shown in Fig. 6 and Fig. 7, respectively. It is worth noting that all retrieves were performed with an assumption of the multiphase sample.
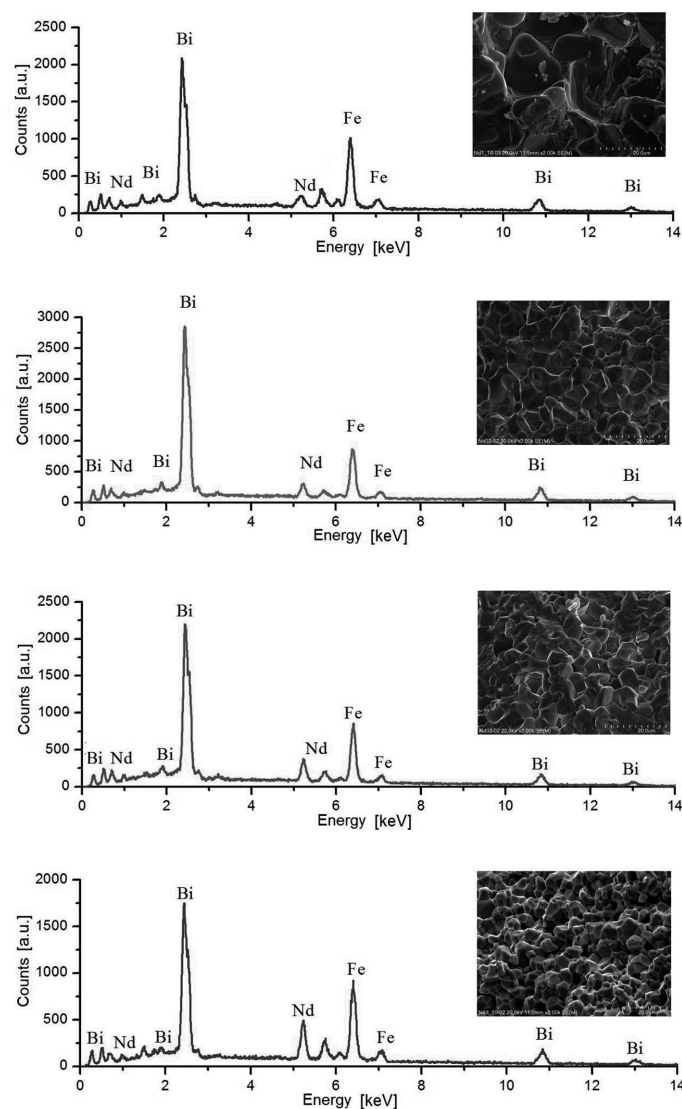

Fig. 5. EDS spectra and SEM photographs of fracture for $Bi_{0.9}Nd_{0.1}FeO_3$ (a), $Bi_{0.8}Nd_{0.2}FeO_3$ (b), $Bi_{0.7}Nd_{0.3}FeO_3$ (c) and $Bi_{0.6}Nd_{0.4}FeO_3$ (d) ceramics

TABLE 1

Theoretical and experimental content of element (calculation for simple oxide) for $Bi_{1-x}Nd_xFeO_3$ ceramics

Formula	Oxide content by EDS measurement [%]			Theoretical content of oxides [%]			Content error [%]		
	Bi_2O_3	Nd_2O_3	Fe_2O_3	Bi_2O_3	Nd_2O_3	Fe_2O_3	Bi_2O_3	Nd_2O_3	Fe_2O_3
$Bi_{0.9}Nd_{0.1}FeO_3$	69.03	5.23	25.72	68.44	5.49	26.06	+0.88	-4.73	-1.30
$Bi_{0.8}Nd_{0.2}FeO_3$	61.25	11.72	27.03	62.15	11.22	26.62	-1.45	+4.46	+1.54
$Bi_{0.7}Nd_{0.3}FeO_3$	56.07	17.00	26.93	55.58	17.20	27.21	+0.88	-1.16	-1.03
$Bi_{0.6}Nd_{0.4}FeO_3$	49.90	22.59	27.51	48.71	23.45	27.82	+2.44	-3.67	-1.11

One can see from Fig. 6 that apart from bismuth iron oxide ($BiFeO_3$; PDF reference code 01-086-1518) and neodymium iron oxide ($NdFeO_3$; PDF reference code 01-089-6644) other phases like tetragonal $Bi_{24}Fe_2O_{39}$ (PDF 00-042-0201) and orthorhombic $Bi_2Fe_4O_9$ (AMCSD entry [18]) are present in the sample. Semi-quantitative calculations based on reference intensity ratio method [19] have shown the following amount of the phases: bismuth iron oxide $BiFeO_3$-63.7%; neodymium iron oxide $NdFeO_3$-17.8%; bismuth iron oxide $Bi_{24}Fe_2O_{39}$-9.5% and $Bi_2Fe_4O_9$-9.0%. In case of $Bi_{0.8}Nd_{0.2}FeO_3$ the calculations resulted in the following amount of the phases: bismuth iron(III) oxide (ICSD-28027) $BiFeO_3$-75.1%; neodymium iron oxide (ICSD-27275) $NdFeO_3$-8.8% and bismuth iron oxide (PDF code 01-082-1316) $Bi_{24}(Bi_{1.04}Fe_{0.84})O_{40}$-16%.
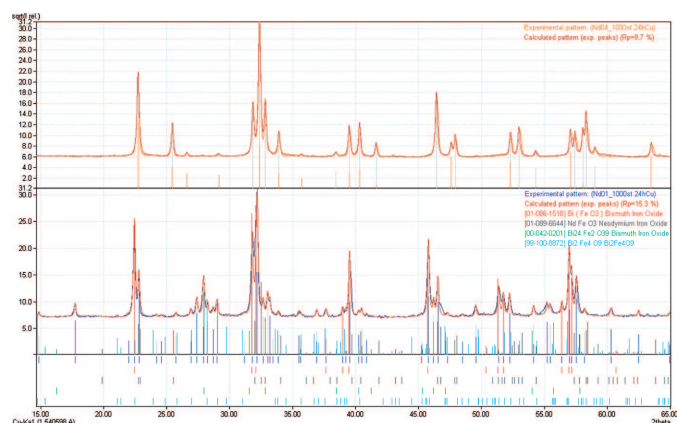

Fig. 6. Results of qualitative X-ray phase analysis of $Bi_{0.9}Nd_{0.1}FeO_3$ powder

Fig. 7. Results of qualitative X-ray phase analysis of $Bi_{0.6}Nd_{0.4}FeO_3$ powder

Results of qualitative calculations performed for $Bi_{0.6}Nd_{0.4}FeO_3$ sample are shown in Fig. 7. One can see from Fig. 7 that only two phases are present in the sample under study, namely bismuth iron oxide ($BiFeO_3$; PDF code 01-086-1518) and neodymium iron oxide ($NdFeO_3$; ICSD collection code 27275). Semi-quantitative calculations yielded rather surprising result, namely the material under study consisted mainly from neodymium iron oxide phase $NdFeO_3$-94.3% with minor amount of bismuth iron oxide $BiFeO_3$-5.7%. It is worth noting that for $Bi_{0.7}Nd_{0.3}FeO_3$ the calculations showed also a phase com-

position with high amount of neodymium iron(III) oxide (ICSD-27275) $NdFeO_3$-86.7%; and bismuth iron(III) oxide (PDF 01-072-2112) $BiFeO_3$-13.3%. The possible explanation of the results of semi-quantitative calculations is that for small concentration of neodymium component (i.e. $x \leqslant 0.2$) $Bi_{1-x}Nd_xFeO_3$ compound adopts rhombohedral structure (i.e. $BiFeO_3$-type structure) while for higher concentrations of neodymium (i.e. $x \geqslant 0.3$) the $Bi_{1-x}Nd_xFeO_3$ compound crystallizes in orthorhombic symmetry (i.e. $NdFeO_3$-type structure).

To verify this hypothesis computer simulation was performed on the basis of crystallographic information files describing rhombohedral $BiFeO_3$ and orthorhombic $NdFeO_3$ compounds. Results of calculations of elementary cell parameters as well as occupancy (SOF – substitution and occupation factor), Wyckoff letters (Wyck), relative atomic coordinates (x,y,z) and isotropic factor B(iso) are given in Tab. 2 – Tab. 5.

TABLE 2

Crystallographic parameters of $Bi_{0.6}Nd_{0.4}FeO_3$ compound

Space group number : 62
Spacegroup : Pnma
Cell choice : 1
Lattice parameter : a =5.6109Å b =7.8057Å c =5.4470Å
Angles : α =90.0° β =90.0° γ =90.0°
Volume of cell : 237.84×10^6 [pm^3]

Name	No.	Ion	Wyck	x	y	z	SOF	B-(iso)
Fe1	26	Fe3+	4b	0.0000	0.0000	0.5000	1.0000	0.7278
Nd1	60	Nd3+	4c	0.0477	0.2500	0.0081	0.3000	0.0000
	83	Bi3+					0.7000	0.0000
O1	8	O2-	8d	0.2753	0.4189	0.2085	1.0000	3.0000
O2	8	O2-	4c	0.5339	0.2500	0.8815	1.0000	2.1091

TABLE 3

Crystallographic parameters of $Bi_{0.7}Nd_{0.3}FeO_3$ compound

Space group number : 62
Spacegroup : Pnma
Cell choice : 1
Lattice parameter : a =5.6111Å b =7.8202Å c =5.4544Å
Angles : α =90.0° β =90.0° γ =90.0°
Volume of cell : 239.34×10^6 [pm^3]

Name	No.	Ion	Wyck	x	y	z	SOF	B-(iso)
Fe1	26	Fe3+	4b	0.0000	0.0000	0.5000	1.0000	0.3712
Nd1	60	Nd3+	4c	0.0459	0.2500	0.9930	0.3000	0.0000
	83	Bi3+					0.7000	0.0000
O1	8	O2-	8d	0.2113	0.5318	0.1824	1.0000	1.3238
O2	8	O2-	4c	0.4950	0.2500	0.0570	1.0000	3.0000

One can see from Tab. 4 and Tab. 5 that for amount of neodymium x =0.1 and x =0.2 crystal structure of the $Bi_{1-x}Nd_xFeO_3$ powder is rhombohedral described with *R3m* (160) space group. On the other hand, for x =0.3 and x =0.4 $Bi_{1-x}Nd_xFeO_3$ compounds adopted orthorhombic symmetry described with *Pnma* (62) space group (Tab. 2 and Tab. 3). With an increase in amount of neodymium parameters of the elementary cell decreased for both structures. Also in case of

$R3m$ (160) space group the rhombohedral distortion of the elementary cell decreased (angles α, β and γ increased).

TABLE 4

Crystallographic parameters of $Bi_{0.8}Nd_{0.2}FeO_3$ compound

Space group number : 160
Spacegroup : R3m
Cell choice : 2
Lattice parameter : $a = 3.9480\text{Å}$ $b = 3.9480\text{Å}$ $c = 3.9480\text{Å}$
Angles : $\alpha = 89.3911°$ $\beta = 89.3911°$ $\gamma = 89.3911°$
Volume of cell : 62.09×10^6 [pm^3]

Name	No.	Ion	Wyck	x	y	z	SOF	B-(iso)
Bi1	83	Bi3+	1a	0.0000	0.0000	0.0000	0.8000	0.0000
	60	Nd3+				1	0.2000	0.0000
Fe1	26	Fe3+	1a	0.5000	0.5000	0.5000	1.0000	0.0000
O1	8	O2-	3b	0.5000	0.5000	0.0000	1.0000	0.0000

TABLE 5

Crystallographic parameters of $Bi_{0.9}Nd_{0.1}FeO_3$ compound

Space group number : 160
Spacegroup : R3m
Cell choice : 2
Lattice parameter : $a = 3.9602\text{Å}$ $b = 3.9602\text{Å}$ $c = 3.9602\text{Å}$
Angles : $\alpha = 89.3636°$ $\beta = 89.3636°$ $\gamma = 89.3636°$
Volume of cell : 61.53×10^6 [pm^3]

Name	No.	Ion	Wyck	x	y	z	SOF	B-(iso)
Bi1	83	Bi3+	1a	1.0000	1.0000	1.0000	0.9000	0.0000
	60	Nd3+					0.1000	0.0000
Fe1	26	Fe3+	1a	0.5000	0.5000	0.5000	1.0000	3.0000
O1	8	O2-	3b	0.5000	0.5000	1.0000	1.0000	3.0000

4. Conclusions

$Bi_{1-x}Nd_xFeO_3$ ceramic powder was synthesized by mixed oxide method from the stoichiometric mixture of oxides, viz Bi_2O_3, Nd_2O_3 and Fe_2O_3. Simultaneous thermal analysis made it possible to determine thermal behavior of $Bi_{1-x}Nd_xFeO_3$ powders. EDS analysis confirmed the chemical composition and purity of the material received. It was found that concentration of neodymium has an effect on particle size. An increase in neodymium content caused a decrease in the average size of the ceramics grains. It was found that crystal structure of $Bi_{1-x}Nd_xFeO_3$ for x$\leqslant$0.2 should be described by rhombohedral symmetry $R3m$ space group (No 160). With an increase in neodymium content both lattice parameters and rhombohedral distortion of the elementary cell decreased. For x$\geqslant$0.3 crystal structure of $Bi_{1-x}Nd_xFeO_3$ was described by orthorhombic symmetry with $Pnma$ (No 62) space group. In this case also the lattice parameters decreased with an increase in neodymium amount. One can conclude that $Bi_{1-x}Nd_xFeO_3$ suffered structural phase transition from rhombohedral to orthorhombic symmetry with an increase in neodymium concentration x within the range x =(0.2-0.3). However, more detailed studies within this range of neodymium concentrations x are necessary.

REFERENCES

[1] J. Wang, J.B. Neaton, H. Zheng, V. Nagarajan, S.B. Ogale, B. Liu, D. Viehland, V. Vaithyanathan, D.G. Schlom, U.V. Waghmare, N.A. Spaldin, K.M. Rabe, M. Wuttig, R. Ramesh, Epitaxial BiFeO$_3$ multiferroic thin film heterostructures, Science **299**, 1719 (2003).

[2] A. Johari, Synthesis and characterization of bismuth ferrite Nnanoparticles, AKGEC Journal of Technology July-December **2**, 2, 0975-9514 (2011).

[3] A. Lisińska-Czekaj, Ł. Madej, J. Plewa, D. Czekaj, Otrzymanie i właściwości magnetyczne ceramiki multiferroicznej BiFeO$_3$, Prace Komisji Nauk Ceramicznych – Polski Biuletyn Ceramiczny Ceramika/Ceramics **101**, 223-228 (2008).

[4] J. Dzik, H. Bernard, K. Osinska, A. Lisinska-Czekaj, D. Czekaj, Synthesis, structure and dielectric properties of Bi$_{1-x}$Nd$_x$FeO$_3$, Archives of Metallurgy and Materials **56**, 4, 1119-1125 (2011).

[5] Z. Dai, Y. Akishige, Electrical properties of multiferroic BiFeO$_3$ ceramics synthesized by spark plasma sintering, Journal of Physics D: Applied Physics **43**, 445403-445407 (2010).

[6] S.M. Selbach, T. Tybell, M.A. Einarsrud, T. Grande, Size- dependent properties of multiferroic BiFeO$_3$ nanoparticles, Chemistry of Materials. **19**, 26, 6478-84 (2007).

[7] Q. Jiang, C. Nan, Y. Wang, Y. Liu, Z. Shen, Synthesis and properties of multiferroic BiFeO$_3$ ceramics, Journal of Electroceramics **21**, 690-693 (2008).

[8] R. Pandu, K.L. Yadav, A. Kumar, P.R. Reddy, A. Gupta, Effect of sintering temperature on structural and electrical properties BiFeO$_3$ multiferroics, Indian Journal of Engeneering & Materials Sciences **17**, 481-485 (2010).

[9] S.H. Han, K.S. Kim, H.G. Kim, H.G. Lee, H.W. Kang, J.S. Kim, Ch.I. Cheon, Synthesis and characterization of multiferroic BiFeO$_3$ powders fabricated by hydrothermal method, Ceramics International **36**, 1365-1372 (2010).

[10] J.K. Kim, S.S. Kim, W.-J. Kim, Sol – gel synthesis and properties of multiferroic BiFeO$_3$, Materials Letters **59**, 4006-4009 (2005).

[11] M.S. Bernardo, T. Jardiel, M. Peiteado, A.C. Caballero, M. Villegas, Reaction pathways in the solid state synthesis of multiferroic BiFeO$_3$, Journal of the European Ceramic Society **31**, 3047-3053 (2011).

[12] B. Wodecka-Dus, J. Dzik, H. Bernard, K. Osinska, A. Lisinska-Czekaj, D. Czekaj, Application of impedance spectroscopy for Bi$_{1-x}$Nd$_x$FeO$_3$ ceramics characterization, Materials Science Forum **730-732**, 71-75 (2013).

[13] G.L. Yuan, O.D. Siu-wing, L. Helen, W. Chan, Raman scattering spectra and ferroelectric properties of Bi$_{1-x}$Nd$_x$FeO$_3$ (x=0–0.2) multiferroic ceramics, Journal of Applied Physics **101**, 064101 (2007).

[14] MATCH! Version 2.x, CRYSTAL IMPACT, Postfach 1251, 53002 Bonn, Germany. (URL.: http://www.crystalimpact.com.matcg)

[15] J. Rodriguez-Carvajal, Physica B. **192**, 55 (1993); http://www.ill.eu/sites/fullprof.

[16] W. K r a u s, G. N o l z e, Powder cell – a program for the representation and manipulation of crystal structures and calculation of the resulting X-ray powder patterns, Journal of Applied Crystallography **29**, 301-303 (1996).

[17] A. L i s i ń s k a - C z e k a j, D. C z e k a j, Synthesis of $Bi_5TiNbWO_{15}$ ceramics, Archives of Metallurgy and Materials **54**, 4, 869-874 (2009).

[18] R.T. D o w n s, M. H a l l - W a l l a c e, The American Mineralogist Crystal Structure Database, American Mineralogist **88** (2003) 247-250; N. N i i z e k i, M. W a c h i, The crystal structures of $Bi_2Mn_4O_{10}$, $Bi_2Al_4O_9$ and $Bi_2Fe_4O_9$, Zeitschrift fur Kristallographie **127**, 173-187 (1968).

[19] C.R. H u b b a r d, E.H. E v a n s, D.K. S m i t h, The reference intensity ratio method for computer simulated powder patterns, J. Appl. Crystallogr. **169**, 9, 169-174 (1976).